ICHEP'98 #416
Submitted to Pa 1
Pl 1

DELPHI 98-100 CONF 168
22 June, 1998

Measurements of the tau leptonic branching ratios

Preliminary

DELPHI Collaboration

K. Johansen [1], V. Lefebure [2], J. M. Lopez [3], F. Matorras [3], M. McCubbin[4], A. Ruiz [3], B. Stugu [1]

Abstract

Using data from 1993 to 1995 measurements of the branching fractions $\tau \to e\nu\bar{\nu}$ and $\tau \to \mu\nu\bar{\nu}$ are presented. The results $B(\tau \to e\nu\bar{\nu}) = (17.98 \pm 0.12_{stat} \pm 0.09_{sys})$ and $B(\tau \to \mu\nu\bar{\nu}) = (17.37 \pm 0.11_{stat} \pm 0.07_{sys})\%$ are obtained. Combined with previously published results based on data from 1991 and 1992, the final DELPHI estimates become: $B(\tau \to e\nu\bar{\nu}) = (17.92 \pm 0.11_{stat} \pm 0.10_{sys})$ and $B(\tau \to \mu\nu\bar{\nu}) = (17.32 \pm 0.10_{stat} \pm 0.07_{sys})\%$,

[1]University of Bergen, Norway
[2]Univ. Instelling, Antwerpen, Belgium
[3]University de Cantalabria, Santander, Spain
[4]University of Liverpool, UK

1 Introduction

A fundamental assumption of the standard model is universality in the charged as well as in the neutral weak currents. The study of τ decays at LEP provides a powerful tool for testing this assumption in the charged current sector. Assuming the neutrino to be massless, the rate for the decay $\tau \to l\nu_\tau\overline{\nu}_l$ can be written as [1]:

$$, (\tau \to l\nu_\tau\overline{\nu}_l) = \frac{G_{l\tau}^2 m_\tau^5}{192\pi} f(x_l) r_{RC} \tag{1}$$

Here, $x_l = \frac{m_l^2}{m_\tau^2}$, $f(x_l)$ is a phase space factor with value $f(x_\mathrm{e}) = 1.0000$ and $f(x_\mu) = 0.9726$. The quantity r_{RC} is a factor due to electroweak radiative corrections, and has the value 0.9960 for both $\tau \to \mathrm{e}\nu\bar{\nu}$ and $\tau \to \mu\nu\bar{\nu}$ decays, and $G_{l\tau}$ is the coupling of the tau to a lepton of type l, and equals the Fermi coupling constant if lepton universality holds.

The branching fractions of the decays $\tau \to \mu\nu\bar{\nu}$ and $\tau \to \mathrm{e}\nu\bar{\nu}$ can be used to test universality in the couplings of the leptons to the weak charged current by computing the ratio of the widths into the two final states:

$$\frac{, (\tau \to \mu\nu\bar{\nu})}{, (\tau \to \mathrm{e}\nu\bar{\nu})} = \frac{g_\mu^2}{g_e^2} \cdot \frac{f(m_\mu^2/m_\tau^2)}{f(m_e^2/m_\tau^2)}, \tag{2}$$

Hence, we have a direct comparison between g_μ and g_e, the couplings of the muon and electron to the charged weak current.

Using τ lifetime and mass measurements together with the leptonic branching ratios, τ - μ universality is tested through the relation:

$$B(\tau \to \mathrm{e}\nu\bar{\nu}) = \frac{g_\tau^2}{g_\mu^2} \cdot \left[\frac{\Delta_{RC}\Delta_f^e}{\tau_\mu}\frac{m_\tau^5}{m_\mu^5}\right] \tau_\tau, \tag{3}$$

where τ_μ and τ_τ are μ and τ lifetimes. The factors Δ_{RC} and Δ_f^e account for differences in electroweak corrections and phase space corrections in $\tau \to \mathrm{e}\nu\bar{\nu}$ as compared to $\mu \to \mathrm{e}\nu\bar{\nu}$. The product $\Delta_{RC} \times \Delta_f$ equals 1.0004.

Similarly, τ - e universality can be tested through the relation:

$$B(\tau \to \mu\nu\bar{\nu}) = \frac{g_\tau^2}{g_e^2} \cdot \left[\frac{\Delta_{RC}\Delta_f^\mu}{\tau_\mu}\frac{m_\tau^5}{m_\mu^5}\right] \tau_\tau, \tag{4}$$

Here Δ_f^μ accounts for phase space corrections in $\tau \to \mu\nu\bar{\nu}$ as compared to $\mu \to \mathrm{e}\nu\bar{\nu}$ and the product $\Delta_{RC} \times \Delta_f^\mu$ equals 0.9731.

In the following, measurements of $B(\tau \to \mathrm{e}\nu\bar{\nu})$ and $B(\tau \to \mu\nu\bar{\nu})$ using data from the DELPHI experiment at LEP collected from 1993 through 1995 are presented. The results are then combined with previously published DELPHI measurements [5] based on 1991 and 1992 data to give the final DELPHI numbers on $B(\tau \to \mathrm{e}\nu\bar{\nu})$ and $B(\tau \to \mu\nu\bar{\nu})$. The measurements are then used to test lepton universality using the formulae above.

2 Method

At LEP, an abundant supply of τ leptons are produced through the reaction $\mathrm{e^+e^-} \to \mathrm{Z^0} \to \tau^+\tau^-$. These events are cleanly separated from other event types, and it turns out

that one can find $\tau^+\tau^-$ selection algorithms with efficiencies which are nearly independent of the specific τ decay mode. Then, the branching fraction for the decay of the τ to lepton l can be measured using the expression

$$B(\tau \to l\nu_\tau\bar{\nu}_l) = \frac{N_l}{N_\tau} \cdot \frac{1-b_l}{1-b_\tau} \cdot \frac{\epsilon_\tau}{\epsilon_l}, \tag{5}$$

where N_l is the number of identified leptonic decays found in the sample of N_τ τ candidates, preselected with efficiency ϵ_τ with a background fraction of b_τ. ϵ_l is the total efficiency for selecting a lepton of type l, with a background fraction of b_l.

For systematic studies, it is useful to factorise ϵ_l into the product $\epsilon_l = \epsilon_\tau^l \times \epsilon_l^{id}$, where ϵ_τ^l is the efficiency for preselecting a τ decaying to a lepton of type l, and ϵ_i^{id} is the efficiency for identifying this lepton, measured with respect to the sample of preselected decays. Then the 'bias factor' defined as $\beta_l = \epsilon_\tau/\epsilon_\tau^l$ is expected to be close to unity for $\tau^+\tau^-$ selection algorithms based on purely topological requirements. Several systematic effects on ϵ_τ might cancel in the ratio β_l. In the expression above, uncertainties due to the $\tau^+\tau^-$ production cross section, the integrated luminosity, and the trigger efficiency do not enter. This also helps reducing the systematic error of the measurements.

The performance of the procedures used to select $\tau \to e\nu\bar{\nu}$ and $\tau \to \mu\nu\bar{\nu}$ decays was studied using simulated events which were passed through a detailed simulation of the detector response and reconstructed with the same program as the real data. The event generators used were: KORALZ [6] with the TAUOLA 2.5 decay package [7] for $e^+e^- \to \tau^+\tau^-$ events, DYMU3 [8] for $e^+e^- \to \mu^+\mu^-$ events, BABAMC [9] for $e^+e^- \to e^+e^-$, JETSET 7.3 [10] for $e^+e^- \to q\bar{q}$ events and the BDK generator [11] for events with four leptons in the final state. Test samples identified in the data and the use of the redundancy between different components of the detector allowed detailed checks of the simulated detector response. With an expected statistical precision well below 1 %, these checks are of vital importance in order to keep the systematic uncertainty below this level, and the procedures used will be detailed in the relevant sections below.

3 The DELPHI detector

A detailed description of the DELPHI detector can be found in [3]. The principal detector components used in this analysis are the tracking devices for charged particle track and momentum reconstruction, the High Density Projection Chamber (the HPC) for for electron and photon identification, and the Hadron CALorimeter (HCAL) and muon chambers for muon identification. The main tracking device in DELPHI is the Time Projection Chamber (the TPC) which is a large drift chamber extending over the radial distance 35cm $< R <$ 111cm. To enhance the precision of the TPC measurement, tracking is supplemented by a vertex detector (the VD) an inner detector (ID) at radii below 35 cm and the Outer detector (the OD) at distances between 198 and 200 cm from the mean axis. The TPC also provides up to 192 ionisation measurements per charged track, useful for electron/hadron separation. The main device for electron identification is the HPC which offers full reconstruction of the longitudinal and transverse components of electromagnetic showers. The HCAL is longitudinally segmented into 4 layers and covers most of the solid angle. Between the third and the fourth HCAL layers and outside the fourth layer, there are chambers for detecting the muons which are expected to penetrate the whole HCAL (the MUB, MUS and the MUF).

4 Initial $e^+e^- \to \tau^+\tau^-$ selection

4.1 Selection criteria

The reaction $e^+e^- \to \tau^+\tau^-$ at LEP energies is characterised by two low multiplicity, highly collimated, back-to-back jets of particles, with significant missing energy due to the undetected neutrinos from the τ decays. The $\tau^+\tau^-$ event selection described here was common to both leptonic decay channels and very similar to previous studies [4].

Each event was divided into hemispheres by a plane perpendicular to the thrust axis, which was calculated using the charged particles. Both hemispheres had to contain at least one charged particle. The highest momentum charged particle in each hemisphere was defined as the leading particle for that hemisphere. At least one of the two leading particles per event had to have a polar angle, θ, with $|\cos\theta| < 0.731$. The point of closest approach of both leading particles from the centre of the interaction region had to be less than 4.5 cm in z and at least one of them had to be within 0.3 cm in the $R\phi$ plane. These cuts removed most of the background from cosmic rays.

The background from hadronic decays of the Z^0 was reduced by asking for a maximum of six charged particles originating from the interaction region.

Events with four fermions in the final state ($e^+e^-e^+e^-, e^+e^-\mu^+\mu^-, e^+e^-\tau^+\tau^-$ and $e^+e^-q\bar{q}$) were rejected by requiring that the isolation angle, defined as the minimum angle between any two charged particles in different hemispheres, had to be greater than 160°. This also reduced the $e^+e^- \to q\bar{q}$ background further. Furthermore, the total energy in the event, E_{vis}, defined as the sum of the neutral electromagnetic energy and the energy of the charged particles, had to be greater than $0.0875 \times E_{cm}$ where E_{cm} is the centre of mass energy. For events with only two charged particle tracks reconstructed, these had to have a total vectorial transverse momentum with respect to the beam axis larger than 0.4 GeV/c.

Most of the Bhabhas were excluded by requiring that $E_{rad} = \sqrt{E_1^2 + E_2^2}$ be less than the beam energy, E_{beam}, and the condition $p_{rad} = \sqrt{p_1^2 + p_2^2}$ being less than the beam momentum ,p_{beam}, removed $e^+e^- \to \mu^+\mu^-$ events as well as much of the Bhabhas remaining. Here, E_1, E_2 are the electromagnetic energies deposited in a cone of half-angle 30° around the leading particle in each hemisphere. The variables p_1, p_2 are the momenta of the leading particle in each hemisphere, in most cases as reconstructed in the tracking devices. An alternative momentum estimate was performed for tracks having a significant energy deposition in the HPC, consistent with that expected from an electron. This estimator was defined as a weighted average between the momentum from the tracking devices and the energy seen in the HPC. This estimator was used in the calculation of p_{rad} whenever the energy deposition in the HPC was at least half the reconstructed momentum and the momentum was larger than 10 GeV.

Finally, in two-prong events, the acollinearity between the two charged particles was required to be greater than 0.5°. This reduced $e^+e^- \to e^+e^-$, $e^+e^- \to \mu^+\mu^-$ and the cosmic background further. The final leading track momentum distribution of the selected tau decay candidates is found to be in reasonable agreement with expectation as shown in fig. 4.

4.1.1 Run quality and fiducial volume

The two decay channels under study depend on different detector elements for proper identification. This leads to a channel dependent requirement to the electric performance of the different detector subsystems. The result is that the $e^+e^- \to \tau^+\tau^-$ selection for electron identification is based on a sample corresponding to a slightly higher integrated luminosity compared to the sample used for muon identification, mainly because the electron identification does not make use of the muon chambers.

However, the electron identification relies on the HPC, and $e^+e^- \to \tau^+\tau^-$ candidates were only accepted for electron identification if at least one of the leading tracks could be extrapolated to a point on the HPC surface more than 1° away from the centre of an azimuthal inter-module boundary, and if the at least one of the tracks was within the HPC and TPC polar angle acceptance of $0.035 < |\cos\theta| < 0.731$.

For muon identification, proper functioning of the muon chambers was required. In addition it was required that at least one track had a polar angle with $|\cos\theta| > 0.035$ for proper reconstruction in the TPC.

Table 1 summarises the results of the $\tau^+\tau^-$ selection.

Channel	$\tau \to \mu\nu\bar{\nu}$	$\tau \to e\nu\bar{\nu}$
Number of τ pairs	68655	68668
Efficiency	52.57 ± 0.04	50.87 ± 0.04
e^+e^-	0.70 ± 0.06	0.65 ± 0.06
$q\bar{q}$	0.68 ± 0.04	0.69 ± 0.04
$\mu^+\mu^-$	0.32 ± 0.01	0.32 ± 0.01
$e^+e^-e^+e^-$	0.70 ± 0.07	0.70 ± 0.07
$e^+e^-\tau^+\tau^-$	0.39 ± 0.04	0.39 ± 0.04
$e^+e^-\mu^+\mu^-$	0.26 ± 0.02	0.26 ± 0.02
cosmics	0.03 ± 0.002	0.03 ± 0.002
Total background	3.09 ± 0.11	3.05 ± 0.11

Table 1: Summary of $\tau^+\tau^-$ selection statistics. The left number is the number obtained for extraction of $B(\tau \to \mu\nu\bar{\nu})$ and the right hand number is that used for $B(\tau \to e\nu\bar{\nu})$. Efficiencies and background levels are in percent. The uncertainties quoted here are from the measurements of the background levels and from simulation statistics. Additional uncertainties are discussed in the text and listed in separate tables for each of the two decay modes.

4.2 Backgrounds in the preselection samples

The backgrounds in the sample add up to about 3 %, and each component must typically be known with a relative precision of 10 % to give a systematic error well below the expected statistical precision of the measurements. Predictions from simulation must be carefully checked, as the backgrounds usually come from tails of distributions, where possible discrepancies between simulation and data are most likely to appear.

The level of the Bhabha and $e^+e^- \to \mu^+\mu^-$ backgrounds were measured by fitting these contributions to the E_{rad} and p_{rad} distributions respectively, when all other cuts in the selection were applied. Fig. 1 shows the E_{rad} and p_{rad} distributions and their comparison with simulation. As discrepancies around the cut values also may stem from inadequate modelling of the response to tau-pairs, the range of the fit is chosen to cover a region dominated by background as indicated on the figure. The fit of the Bhabha contribution to E_{rad} had a χ^2 of 2.4 for 9 degrees of freedom and gave an uncertainty in the Bhabha background of 7%. Similarly, the fit of the muon pair contribution to p_{rad} had a χ^2 of 4.9 for 9 degrees of freedom with an uncertainty in the background of 3%.

A similar procedure was chosen to check the level of the $e^+e^- \to q\bar{q}$ background. Selecting events with charged particle multiplicity of 5 or 6 gave a sample enhanced with $e^+e^- \to q\bar{q}$ events. For this sample of events, the isolation angle distribution was dominated by $e^+e^- \to q\bar{q}$ events for the region between 120 and 150 degrees, the other main contribution being $\tau^+\tau^-$ events. The level of the $e^+e^- \to q\bar{q}$ background was adjusted to fit the fraction of events seen in this region with respect to the number seen in the region 120 to 180 degreees. The agreement with the pure simulation estimate was relatively good, adjustments between 2 and 8 % of this estimate were required (depending on which year the data were taken). Fig. 2 shows the distribution of the isolation angle.

To verify the four fermion background the momentum distribution of electrons and muons was studied when the isolation angle requirement was not applied. It was found that the contribution from $e^+e^-\tau^+\tau^-$ events was significant, and had to be accounted for to get a satisfactory description of the final momentum distributions in the two channels. No further cuts against this background are made in the muon analysis, and just one cut against this is made for the electron analysis with a large reduction in the $e^+e^- \to e^+e^-$ background, but with little effect on the final branching ratio estimate. It was thus assumed that corrections to the background level deduced could be applied equally well to the preselection sample. The background due to $e^+e^-q\bar{q}$ events was found to be neglible, as the isolation angle for these events are generally much smaller than 160 degrees.

The level of cosmic ray events in the sample is estimated by studying the impact parameter distribution. Plotting r_1 versus r_2, where r_1 and r_2 are the impact parameters of the leading track of each hemisphere, the cosmic ray events are clearly observed as a diagonal band (fig. 3). The density of events in this band was used to estimate the amount of cosmic ray events satisfying the impact parameter requirements.

4.3 Efficiency of the preselection sample

Having adjusted the backgrounds, the efficiency of a given cut was checked by by comparing the number of events rejected by a given cut in data to the corresponding number from simulation. These numbers were background substracted to get efficiency estimates, ϵ_{data} and ϵ_{mc}. The differences observed are taken as estimates of the systematic uncertainties associated to the efficiencies of the cuts. For the isolation angle cut, only the region with isolation angle larger than 140 degrees was considered, as the distribution at smaller isolation angles is dominated by $e^+e^-q\bar{q}$ events, a background which is not present in the final sample.

As noted, it is the way the bias factor, β_l, is affected by an uncertainty in ϵ_τ which is relevant for the systematic uncertainty in the branching ratio. To estimate this dependence, the change in β_l for a given change in efficiency was computed cut by cut by

Cut	$\epsilon_{data}/\epsilon_{mc}$	$\frac{\Delta\beta_e/\beta_e}{\Delta\epsilon_\tau/\epsilon_\tau}$	$\sigma(\beta_e)/\beta_e$ (%)	$\frac{\Delta\beta_\mu/\beta_\mu}{\Delta\epsilon_\tau/\epsilon_\tau}$	$\sigma(\beta_\mu)/\beta_\mu$ (%)
E_{rad}	0.996	0.17	0.07	-0.68	0.27
P_{rad}	0.992	-0.11	0.09	0.04	0.03
Isolation angle	0.992	0.08	0.06	-0.27	0.02
Visible energy	0.999	0.91	0.07	1.00	0.08
Acolinearity	0.999	0.19	0.01	0.35	0.03
Missing p_t	0.998	0.25	0.05	0.15	0.04
Total systematic			0.16		0.29

Table 2: Dependence of the bias factor, β_l for a change in efficiency for a given cut, and resulting systematic error on the bias factor (in percent for $\tau \to e\nu\bar{\nu}$ and $\tau \to \mu\nu\bar{\nu}$ respectively)

varying the location of the cut around the chosen value. Then the relative systematic uncertainty on β_l was computed as the product between this 'derivative' and the systematic uncertainty in the efficiency as defined above. Table 2 summarizes the results of this study.

5 Analysis of $\tau \to \mu\nu\bar{\nu}$ decays

5.1 Identification requirements

Muons were selected with very high efficiency by requiring that the muon candidate satisfied at least one of the following conditions: either 1) No single HCAL layer should have more than 3 GeV of deposited energy while the outermost layer should have at least 0.2 GeV, or 2) at least two hits in the muon chambers should be associated to the track. Both these requirements reject hadrons with high power while maintaining a good efficiency to muons. Asking that at least one of the two requirements be satisfied results in a selection of muons with very high efficiency. The efficiency of the muon identification drops steeply for momenta below 2 GeV, and to obtain an even and high efficiency it was required that the track momentum should be larger than 0.05 $\times$ the beam momentum. Distributions of the relevant identification variables are shown in fig. 5. The data/simulation agreement is not perfect, and correction procedures are defined as described in section 5.2 below. It was also required that only one charged particle should be present in the hemisphere, consistent with expectation for the $\tau \to \mu\nu\bar{\nu}$ decay.

Two further requirements were imposed in order to suppress $e^+e^- \to \mu^+\mu^-$ events: if a muon was identified in each hemisphere it was required that the total visible energy in the event should be less that 0.7 $\times$ the centre of mass energy. Furthermore the total energy seen in the hemisphere opposite to the $\tau \to \mu\nu\bar{\nu}$ candidate should be less than 0.8 $\times E_{beam}$. To supress charged hadrons misidentified as muons it was required that the average energy deposit per HCAL layer be less that 2 GeV. Furthermore, as these hadrons very often are accompanied by one or more π^0s, it was required that the sum of the assocated and neutral electromagnetic energy in an 18 degree cone around the track should be less than 3 GeV.

5.2 Efficiency measurement

The redundancy between the HCAL and the muon chamber identification permits comparisons between efficiency estimates deduced from data with the same estimates from simulation. As fig. 8 shows, this results in a correction to the efficiency - something which is not surprising in view of the disagreements observed in the identification variables (fig. 5). The estimated identification efficiency of $(97.72 \pm 0.06)\%$ within the momentum and angular acceptance from this redundancy requirement is only valid for muons reaching the outer parts of the detector. $e^+e^- \to \mu^+\mu^-$ events were used to verify the correctness of the efficiency as estimated from simulation (after applying the correction).

The requirements designed to reduce external and internal backgrounds make use of the HPC and the HCAL, but not the muon chambers. The efficiency of these requirements could thus be measured using a very clean sample of muons selected using the muon chambers with tight requirements to observed hit pattern. The resulting sample consisted of about half the total number of $\tau \to \mu\nu\bar{\nu}$ candidates and was nearly background free. The efficiency of the multiplicity requirement was also measured using this sample. Total corrections at the level of 0.2 to 0.4 percent (dependent of the year) were deduced. The precision of these efficiency corrections combine into a systematic uncertainty of 0.2 %. Finally, the efficiency of the requirements to remove $e^+e^- \to \mu^+\mu^-$ events was verified by comparing the number of events rejected in the data to the number rejected by simulation.

The identification efficiency with respect to the preselection sample is estimated at $\epsilon^l_{id} = (82.70 \pm 0.20)\%$. Around half of the losses is due to the momentum cut, while the rest come from the identification and background suppression requirements. The final $\tau \to \mu\nu\bar{\nu}$ selection efficiency with respect to the full solid angle , ϵ_μ, was $(46.12 \pm 0.11)\%$.

5.3 Background measurements

Backgrounds from four fermion final states ($e^+e^-\tau^+\tau^-$ and $e^+e^-\mu^+\mu^-$) were determined from simulation and the level was verified by studying the momentum distribution when the isolation angle requirement was not applied. An adjustment upwards of the level by 10 % was found to improve the agreement between simulation and data. The $\mu^+\mu^-$ background level was measured by studying the momentum distribution of selected muon candidates when the p_{rad} cut was not imposed. The high level of background seen in fig. 6 is well reproduced by simulation, giving confidence that estimates of the much reduced background levels in the final sample are correct within the uncertainties assigned.

The background of τs decaying to hadrons was measured by selecting one track τ decay candidates with a cone energy larger than 3 GeV. This selects final states with one or more neutral pions present, in additon to the charged particle. This sample of events was subjected to the complete analysis (with the exception of the cone energy requirement), and the remaining sample was used to measure the background from this source. Fig. 7 shows the momentum distribution of the selected sample. After scaling up the contribution from hadrons the momentum distribution was found to agree well with expectation from simulation. Good agreement was also found in the tails of the distributions of the cone energy as well as in the HCAL energy depositions, after applying the same scale factor to the background contribution to these plots.

Fig. 9 shows the final momentum distribution compared to expectation. The results of the identification are shown in table 3.

Number of $\tau \to \mu\nu\bar{\nu}$ candidates	21040
Efficiency	46.12 ± 0.11
Total background	3.65 ± 0.16
Taus not decaying to muons	1.40 ± 0.08
$\mu^+\mu^-$	0.33 ± 0.03
$e^+e^-\mu^+\mu^-$	1.31 ± 0.13
$e^+e^-\tau^+\tau^-$	0.43 ± 0.04
cosmics	0.17 ± 0.01

Table 3: Number of $\tau \to \mu\nu\bar{\nu}$ candidates, selection efficiency and background estimates (in percent). The uncertainty in efficiency quoted here is the contribution coming from the identification procedure. Uncertainties in the backgrounds are from simulation, cross checks and measurements of background levels.

Additional studies were performed to estimate the systematic uncertainties coming from uncertainties on the τ branching ratios, the τ polarisation and from the precision of the knowledge of the momentum scale and resolution. The systematic uncertainties are listed in table 4.

Preselection efficiency (i.e. uncertainty in β_l)	0.050
Muon selection efficiency	0.040
Backgrounds in the muon sample	0.023
Backgrounds in the preselection sample	0.016
Uncertainties in the tau branching fractions	0.004
Momentum scale	0.003
Scale differences between positive and negative tracks	0.009
Momentum resolution	0.006
Uncertainty in polarisation	0.002
total systematics	0.071

Table 4: Summary of the absolute uncertainties $\times 100$ on the $\tau \to \mu\nu\bar{\nu}$ branching fraction measurements.

6 Analysis of $\tau \to e\nu\bar{\nu}$ decays

6.1 Electron identification

The main variables used for electron identification were the dE/dx measurement in the TPC (where a minimum of 38 anode sense wires was required to have a signal recorded), and the ratio between the electromagnetic energy deposited in the HPC and the momentum reconstructed in the tracking devices. For both these quantities, pull variables were

constructed which were based on the measured value of the variable, its resolution and the value expected for a given particle type. The variables $\Pi^{e}_{dE/dx}$ and $\Pi_{E/p}$ are defined as the signed number of standard deviations by which the measured value differed from the expectation for an electron. For efficient rejection of pions at the lower half of the momentum spectrum, a similar variable, $\Pi^{\pi}_{dE/dx}$, was defined where the energy loss expectation is that given by the pion hypothesis. The inputs to the pull variables were studied as a function of momentum and of angle, tuning the response simulated to agree with observation in the data. It was observed that the energy deposition by hadron showers starting before or inside the HPC had to be scaled down by abaout 10 % in the simulation to get good agreement with data, possibly due to an underestimate of the nuclear interaction length of the material in some of the subdetectors. Such a hypothesis is also consistent with the corrections needed to the levels of backgrounds as estimated from simulation (see discussion below).

For a particle to be identified as coming from the decay $\tau \to e\nu\bar{\nu}$ it had to be the only charged particle in the hemisphere, and have a momentum greater than $0.01 \times p_{beam}$. To ensure a high and even efficiency over the whole momentum range, the data were divided into three groups in momentum, with different identification criteria applied. For $0.05 < p/p_{beam} < 0.5$, two identification reuquirements could be defined. Firstly the dE/dx information could be used by requiring $\Pi^{\pi}_{dE/dx} > 3$. Secondly, electromagnetic energy deposition was used by requiring $\Pi_{E/p} > -1.5$. To get a very high and even efficiency, it was required that at least one of these criteria should be fulfilled. Fig. 10 shows the two pull variable distributions in the relevant region of electron momentum. For momenta above $0.5 \times p_{beam}$ it was required that $\Pi_{E/p}$ be larger than -1.5 (fig. 11 a). The efficiency of this requirement was verified using Bhabhas and good agreement between data and simulation was found. Finally, for the whole momentum range, the dE/dx was required to be compatible with expectation for an electron by demanding that $\Pi^{e}_{dE/dx}$ be greater than -2. This reduced the background from hadrons and muons, especially at low momenta, while keeping about 97 % of the electrons.

The residual backgrounds from hadronic τ decays were reduced by vetoing decays with energy deposited beyond the first layer of the HCAL. It was also required that there should be no neutral electromagnetic shower with an energy greater than 4 GeV inside a cone of half-angle 18° around the particle. Showers originating from neutral particles within 1° in polar angle of the track, which appeared to originate from bremsstrahlung, were excluded from the calculation of the cone energy.

Electron backgrounds from $e^+e^- \to (e^+e^-)e^+e^-$ interactions were effectively reduced for two particle events where both momenta were less than $0.2 \times p_{beam}$ by requiring that the measured dE/dx for the track in the opposite hemisphere be inconsistent with the value expected for an electron, requiring $\Pi^{\pi}_{dE/dx} < 2$.

There were 18273 $\tau \to e\nu\bar{\nu}$ decays identified. The momentum distribution is found to agree well with expectation from simulation as shown in fig. 12. The identification efficiency and backgrounds are summarised in Table 5, and discussed below.

6.2 Efficiency measurement

The redundancy of the dE/dx and the E/p requirements allows detailed studies of efficiencies and backgrounds. Fig. 13 shows, as an example, the result of such a consistency check for the 1994 data. Corrections are applied bin by bin to get an overall correction

to the efficiency of the requirement. The identification efficiency from simulation was checked at high energies using $Z^0 \to e^+e^-$ events, and it was found that a correction to the efficiency estimate from simulation due to the $\Pi^e_{dE/dx}$ requirement had to be applied. For the years 1994 and 1995 the tails were more significant in the simulation than in the data, resulting in an upwards change in the identification efficiency estimate for these years of about 1.7 %. The study of this distribution for 1993 resulted in a downward change in the efficiency of about 1.0 %. As the dE/dx response to electrons is expected to saturate the relativistic limit for the whole momentum range, this discrepancy lead to an overall correction. It was verified that the $\Pi^e_{dE/dx}$ distributions for simulated $\tau \to e\nu\bar{\nu}$ decays were compatible with that found for simulated Babhas.

To study the efficiency of the multiplicity requirement as well as the requirements applied to reject hadrons (HPC cone energy and energy deposition in the HCAL), a very clean sample of about half the electron candidates was selected by tightening the dE/dx requirement to $\Pi^e_{dE/dx} > 0$. This lead to direct measurements of the efficiency of these cuts, as well as of the multiplicity requirement by comparing the number of events rejected to the corresponding simulation estimate. The electron identification efficiency, ϵ_l, was $(72.30 \pm 0.29)\%$ when measured with respect to the sample of preselected τ decays.

6.3 Background estimates

The background due to $e^+e^- \to e^+e^-$ and $e^+e^- \to (e^+e^-)e^+e^-$ events was verified by studying the momentum distribution of identified electrons when cuts designed to reject these backgrounds were not applied. As fig. 14 shows, the agreement of the backround levels is still good, giving confidence in the estimates.

For reconstructed momenta below half the beam momentum, the background level from hadrons was estimated by adjusting the tail of the $\Pi^e_{dE/dx}$ to fit observation in data. For larger momenta, the background contribution to the tail of the $\Pi_{E/p}$ distribution was adjusted to fit the amount observed in the data. Both these adjustments lead to a significant downscaling of the background relative to the simulation result. Furthermore it was observed that there was *less* background rejected by the HCAL requirement in simulation compared with data. This can be understood if too few hadrons reach the HCAL in simulation, resulting in more events to be rejected by the TPC and the HPC requirements, exactly as observed.

The background fraction for the $\tau \to e\nu\bar{\nu}$ decay sample, b_l, was found to be 5.23 ± 0.30.

7 Results and Discussion

Using data from 1993 to 1995 the following branching ratios were measured:

$$B(\tau \to e\nu\bar{\nu}) = (17.98 \pm 0.12_{stat} \pm 0.09_{sys})\%.$$

$$B(\tau \to \mu\nu\bar{\nu}) = (17.37 \pm 0.11_{stat} \pm 0.07_{sys})\%.$$

The result is in agreement with the current world average values [2], and in reasonable agreement with previously published DELPHI results [5] which used data from the years

Number of $\tau \to e\nu\bar{\nu}$ candidates	18273
Total efficiency	36.79 ± 0.14
Total background	5.23 ± 0.30
τ not decaying to muons	2.11 ± 0.21
e^+e^-	1.92 ± 0.19
$e^+e^-e^+e^-$	0.79 ± 0.08
$e^+e^-\tau^+\tau^-$	0.42 ± 0.04

Table 5: Number of $\tau \to e\nu\bar{\nu}$ candidates, selection efficiency and background estimates (in percent).

Preselection efficiency (i.e. uncertainty in β_l)	0.028
Electron selection efficiency	0.071
Backgrounds in the electron sample	0.049
Backgrounds in the preselection sample	0.016
Uncertainties in the tau branching fractions	0.004
Momentum scale	0.004
Scale differences between positive and negative tracks	0.015
Momentum resolution	0.006
Uncertainty in polarisation	0.002
total systematics	0.094

Table 6: Summary of the absolute uncertainties $\times 100$ on the $\tau \to e\nu\bar{\nu}$ branching fraction measurement.

1991 and 1992. Combining the results obtained here with the results from [5], yields the values:

$$B(\tau \to \mathrm{e}\nu\bar{\nu}) = (17.916 \pm 0.109_{stat} \pm 0.095_{sys})\%.$$

$$B(\tau \to \mu\nu\bar{\nu}) = (17.315 \pm 0.095_{stat} \pm 0.073_{sys})\%.$$

which supersedes all previously published DELPHI measurements.

A test of e-μ universality in the weak charged current can be performed using Eqn. 2. From the 93-95 data , the ratio between the muon and the electron couplings to the charged weak current is estimated to be $\frac{g_\mu}{g_e} = 0.9966 \pm 0.0057$,. This result assumes that the common systematic uncertainty in the two measurements has the value 0.016 (in units of 100 times the quoted result). Combining this with the estimate $\frac{g_\mu}{g_e} = 1.000 \pm 0.013$ from [5] , the final result

$$\frac{g_\mu}{g_e} = 0.9971 \pm 0.0052$$

is obtained.

To test $\tau - \mu$ and $\tau -$ e universality, the preliminary DELPHI value for the τ lifetime of (292.7 ± 2.1) fs [12] is used together with world average [2] values for the τ and muon mass and the muon lifetime. Then, equations 3 and 4 yield

$$\frac{g_\tau}{g_\mu} = 0.9995 \pm 0.0054$$

$$\frac{g_\tau}{g_e} = 0.9963 \pm 0.0054$$

The uncertainty in these estimates are dominated by the the uncertainty in the lifetime (± 0.0036) and the branching ratio measurements (± 0.0040 and ± 0.0035 respectively).

Under the assumption of e-μ universality, $g_\mu = g_e \equiv g_{\mathrm{e},\mu}$, it is possible to give a more stringent test of universality between g_τ and the couplings to two lighter leptons. We combine the two leptonic branching ratios into one leptonic branching ratio, $B_{\mathrm{e},\mu}$, correcting for the phase space suppression of $B(\tau \to \mu\nu\bar{\nu})$:

$$B_{\mathrm{e},\mu} = (17.849 \pm 0.072_{stat} \pm 0.058_{sys})\%.$$

to compare the τ charged current coupling to that of the two lighter leptons. The result

$$\frac{g_\tau}{g_{\mathrm{e},\mu}} = 0.9994 \pm 0.0044$$

is obtained, in excellent agreement with τ-μ-e universality.

Acknowledgements

We are greatly indebted to our technical collaborators and to the funding agencies for their support in building and operating the DELPHI detector, and to the members of the CERN-SL Division for the excellent performance of the LEP collider.

References

[1] W. Marciano and A. Sirlin, Phys. Rev. Lett. **61** (1988) 1815.

[2] Particle Data Group, Phys. Rev. **D54** (1996) 1.

[3] DELPHI collaboration, P.Aarnio et al., NIM A303 (1991) 233.
DELPHI Collaboration, P.Abreu et al., NIM A378 (1996) 57.

[4] DELPHI Collaboration, P.Abreu et al., Nucl. Phys. **B417** (1994) 3.

[5] DELPHI Collaboration, P.Abreu et al., Phys. Lett. **B 357** (1995) 715.

[6] S.Jadach, J.H. Kühn, Z. Was, Comp. Phys. Comm. 79 (1994) 503.

[7] S. Jadach, Z. WAs, R.Decker, J.H. Kühn, Comp. Phys. Comm. 76 (1993) 361.

[8] J.E. Campagne and R. Zitoun, Z.Phys. C43 (1983) 469.

[9] F.A.Berends, W.Hollik, R.Kleiss, Nucl. Phys. B304 (1988) 712.

[10] T.Sjöstrand, Comp,Phys. Comm. 82(1994)74.

[11] F. A. Berends, P. H. Daverveldt, R. Kleiss: "Monte Carlo Simulation of Two-Photon Processes", Comp. Phys. Comm. 40 (1986) 271-284, 285-307, 309-326.

[12] DELPHI contributed paper to HEP'97 (Jerusalem)
DELPHI note 97-87 CONF 73

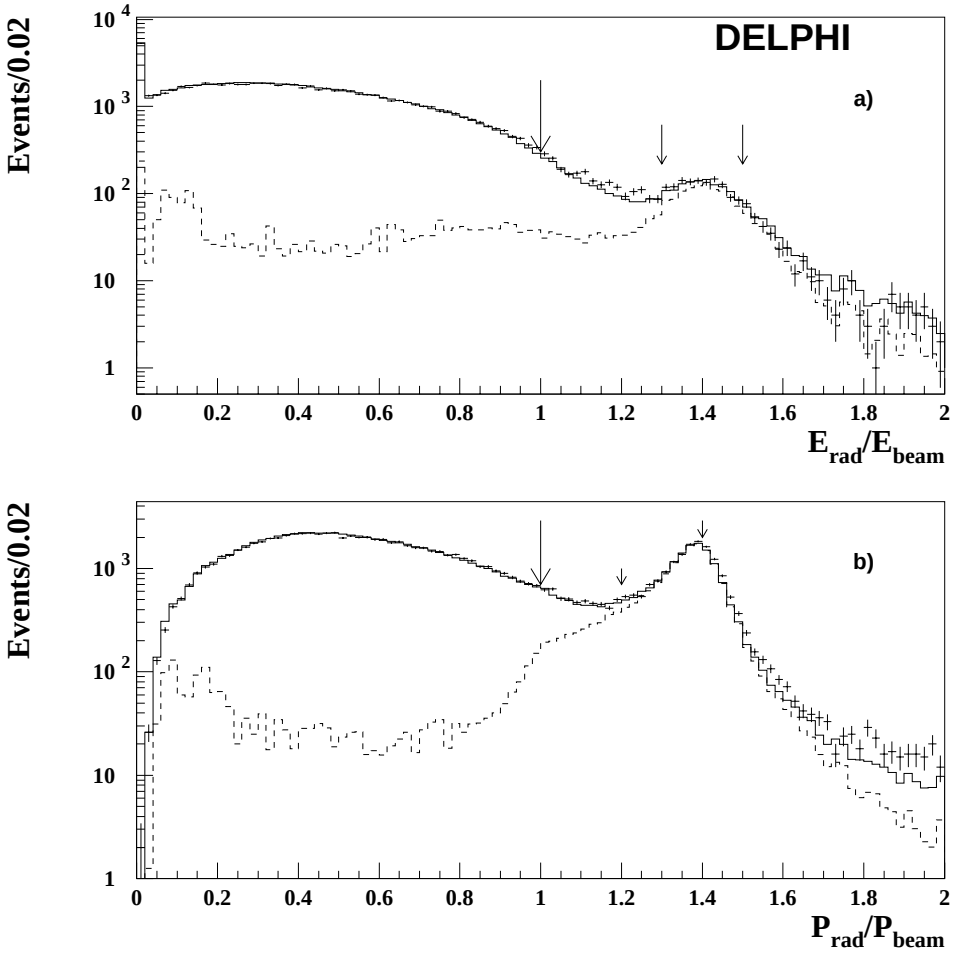

Figure 1: Distribution of a) E_{rad} and b) p_{rad} when these cuts are not applied. The line is expectation from simulation, the dashed line is the expected background contribution. The large arrow shows the cut value, the two smaller ones indicate the range used for normalisation of the background.

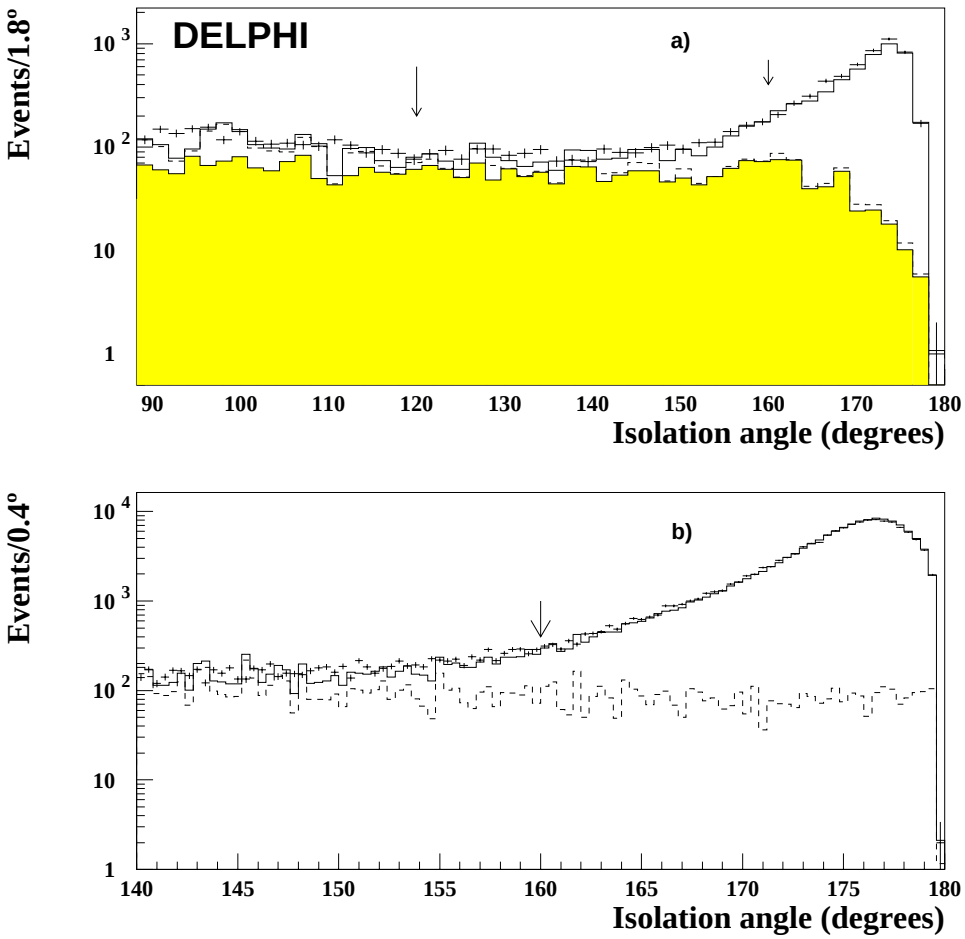

Figure 2: Distribution of the isolation angle when this cut is not applied, a) For events with charged track multiplicity of five or six. The arrows shows the range use to normalise the $q\bar{q}$ background. b) for all eventsi, The arrow indicates the cut value. The line is expectation from simulation, the dashed line is the expected background contribution. The shaded region in figure a) is the expected contribution from $q\bar{q}$ events.

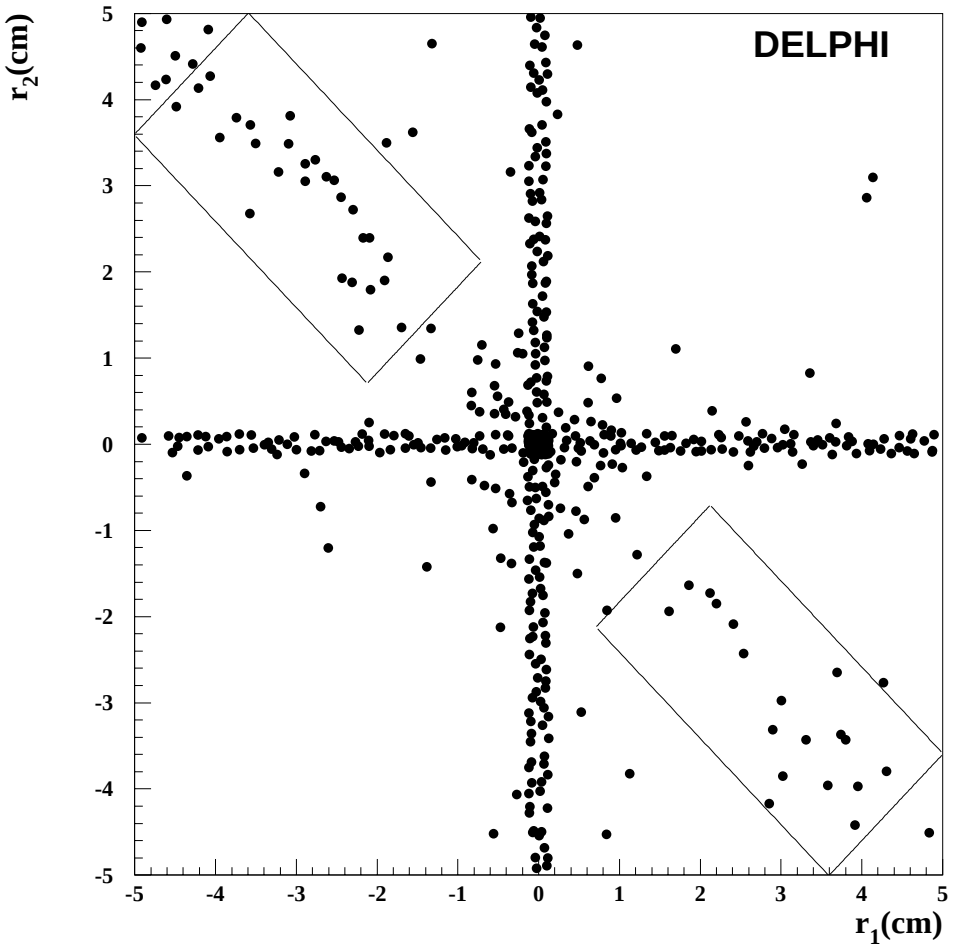

Figure 3: The impact parameter of the leading track in one hemsiphere plotted against the impact parameter of the leading track in the other hemsiphere.

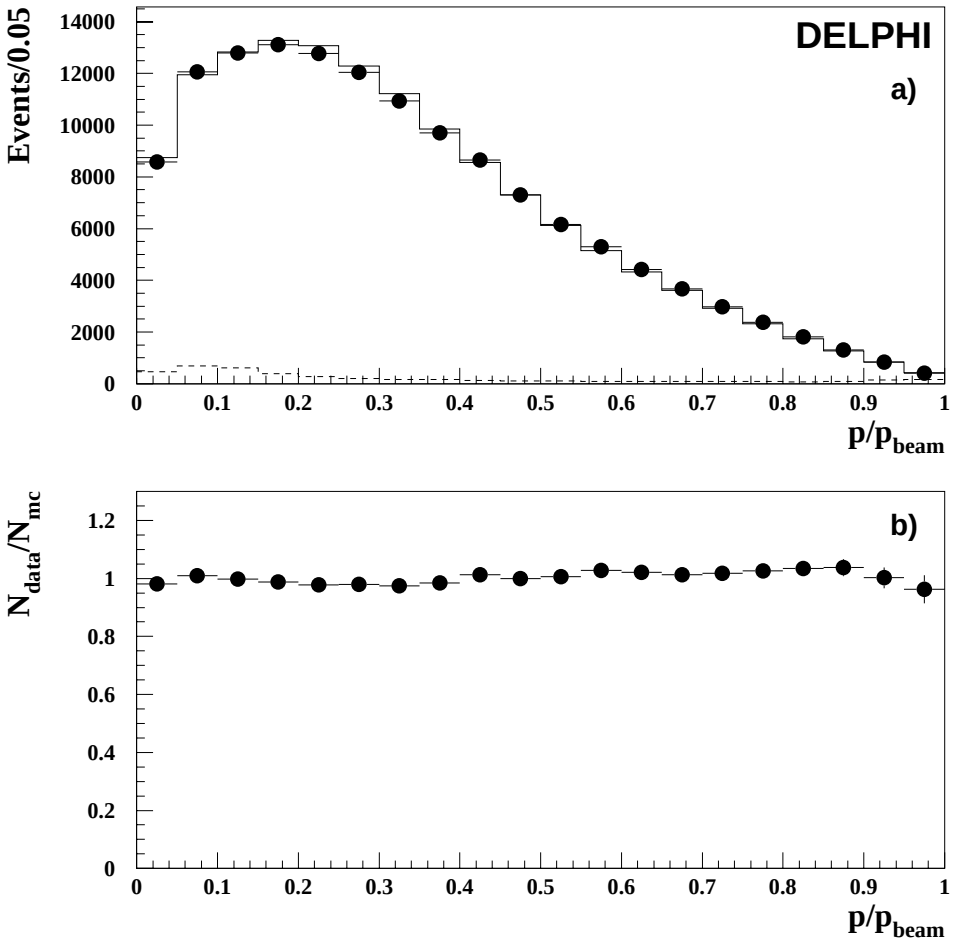

Figure 4: a) Distribution of the leading track momentum of selected τ decays (points) compared to expectation from simulation (line). b) The ratio between data and simulation

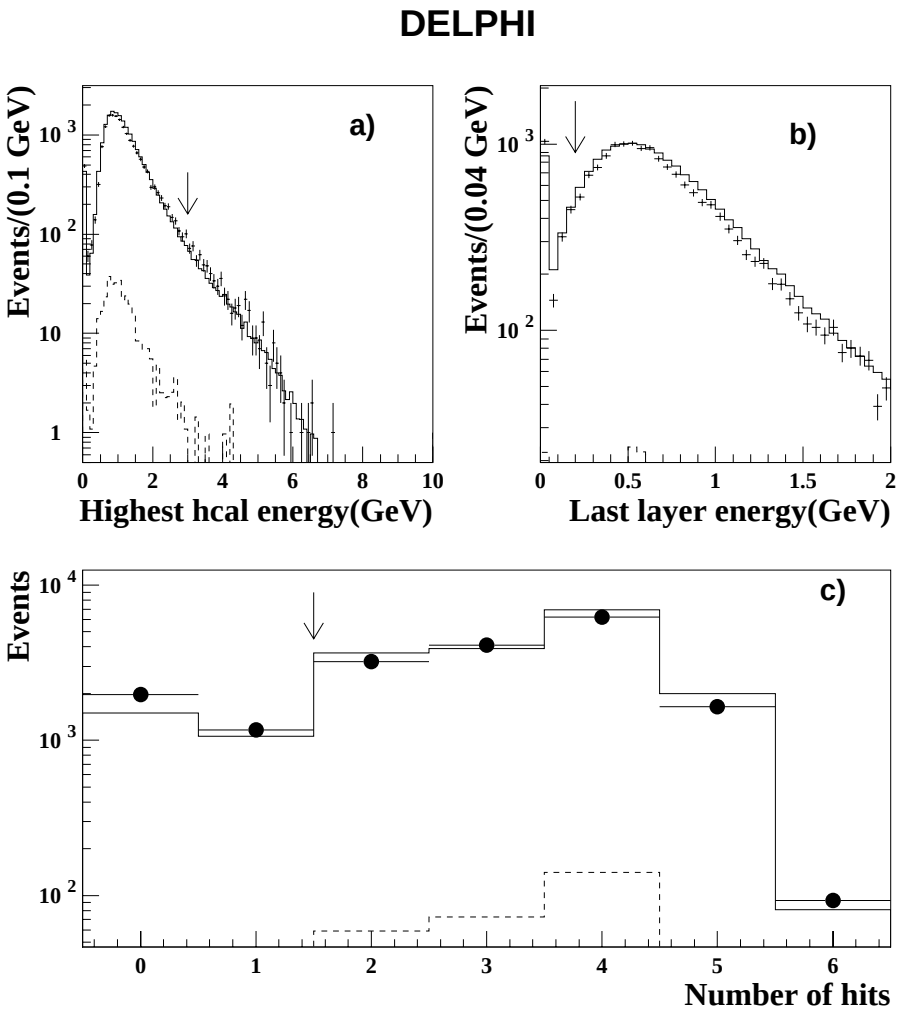

Figure 5: Muon identification variables: Largest HCAL energy deposition (required to be less than 3 GeV); the energy of the outermost HCAL layer (required to be larger than 0.2 GeV), and the number of associated hits in the muon chambers (required to be two or larger). Points are data, solid line is simulation. The muon chamber requirement is applied before plotting the HCAL variables, and the HCAL requirements are applied before plotting the muon chamber hit distribution. The discrepancies in the distributions lead to corrections to the simulated identification efficiency (see text).

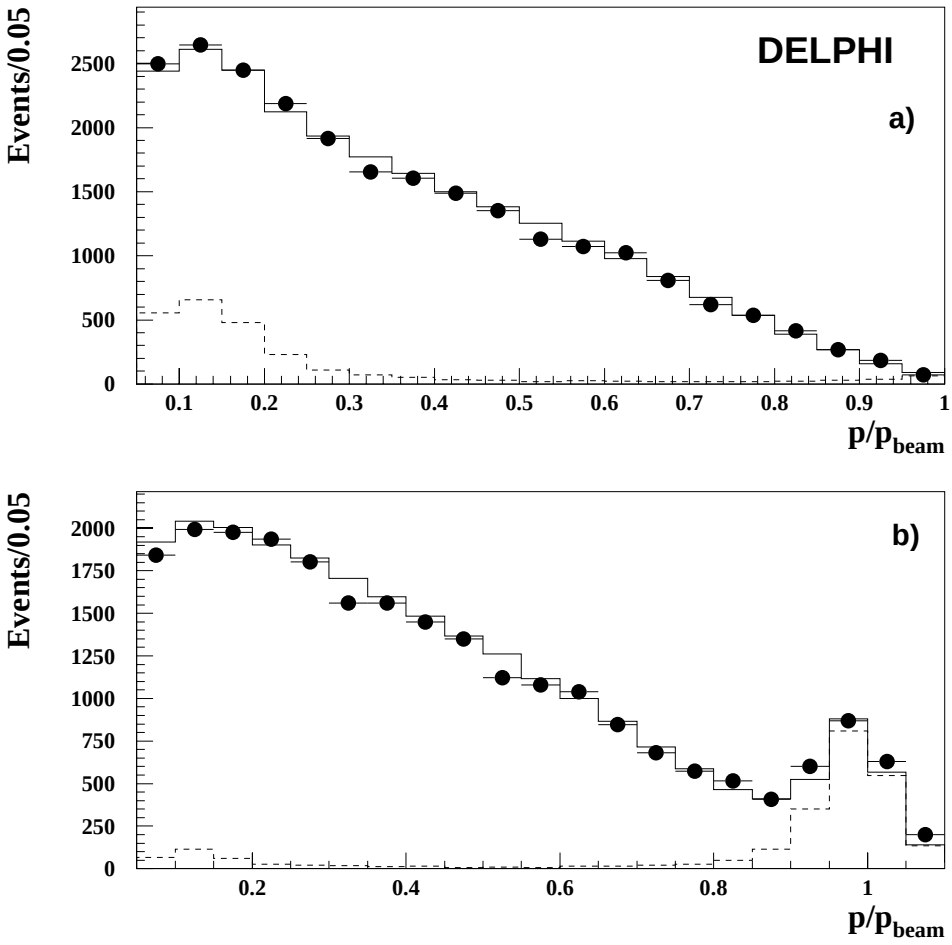

Figure 6: Momentum distribution of the sample of μ candidates when all requirements of the analysis are applied except: a) the isolation angle criterion; b) the p_{rad} requirement. The solid line shows the expectation from simulation.The dashed line shows the expected background contamination.

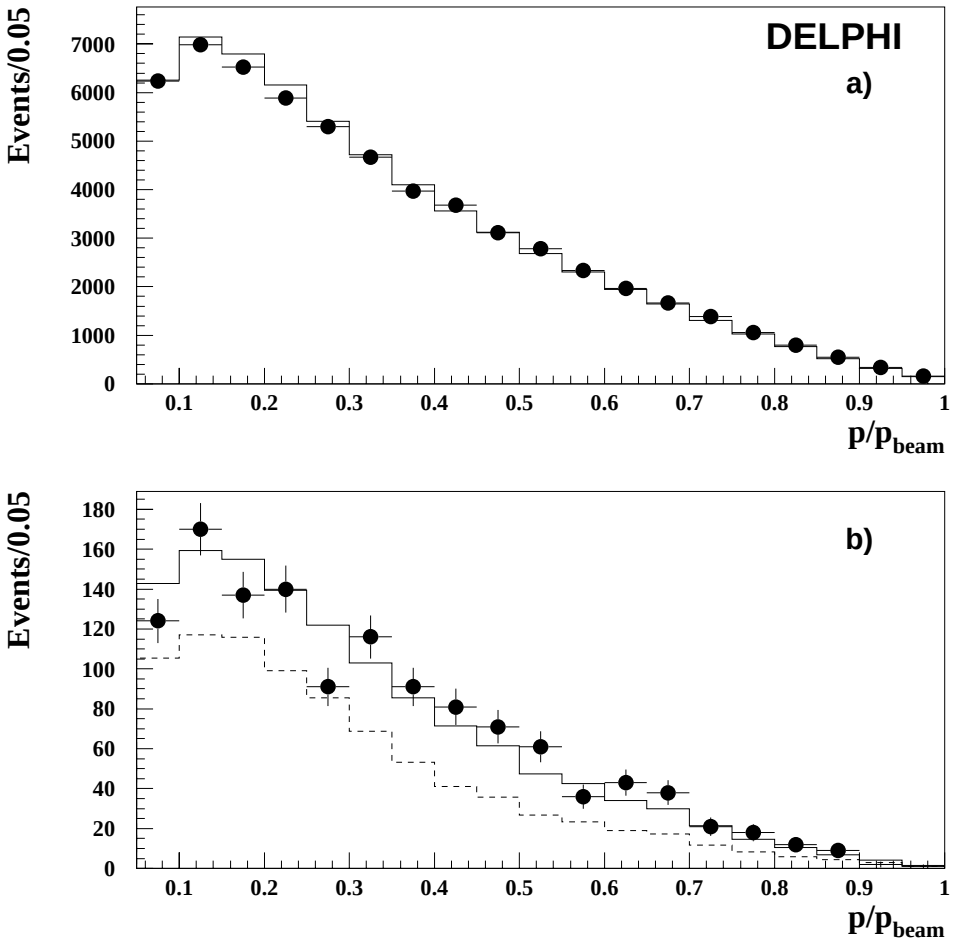

Figure 7: Momentum distribution of a sample of τ decay candidates (almost) not containing muons: a) Initial sample, b) remaining sample satisfying all muon identification requirement except the E_{cone} requirement. The dashed line is the expected non-mu contribution to the distribution after an overall adjustment of the contribution. The solid line is the resulting expectation.

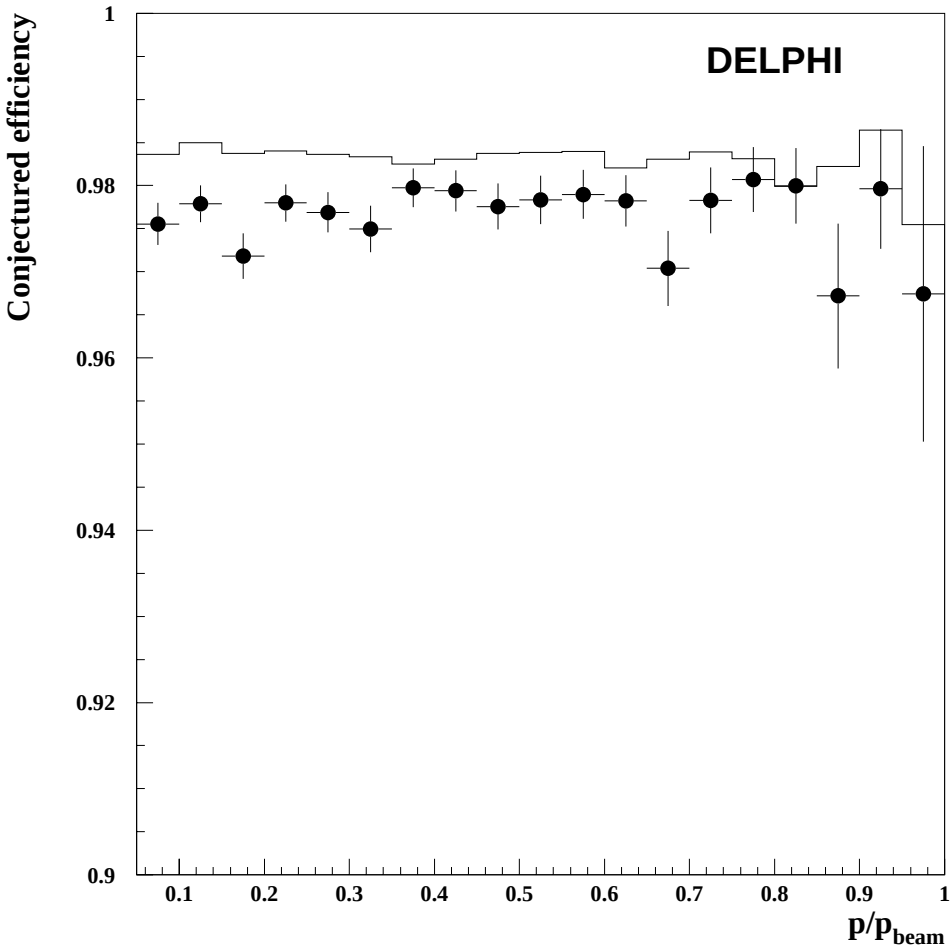

Figure 8: Comparison of data (points) and simulation (solid line) for the estimate of the identification efficiency by measuring the efficiency of the muon chamber requirement with respect to the HCAL requirement. A correction to the simulation result is computed.

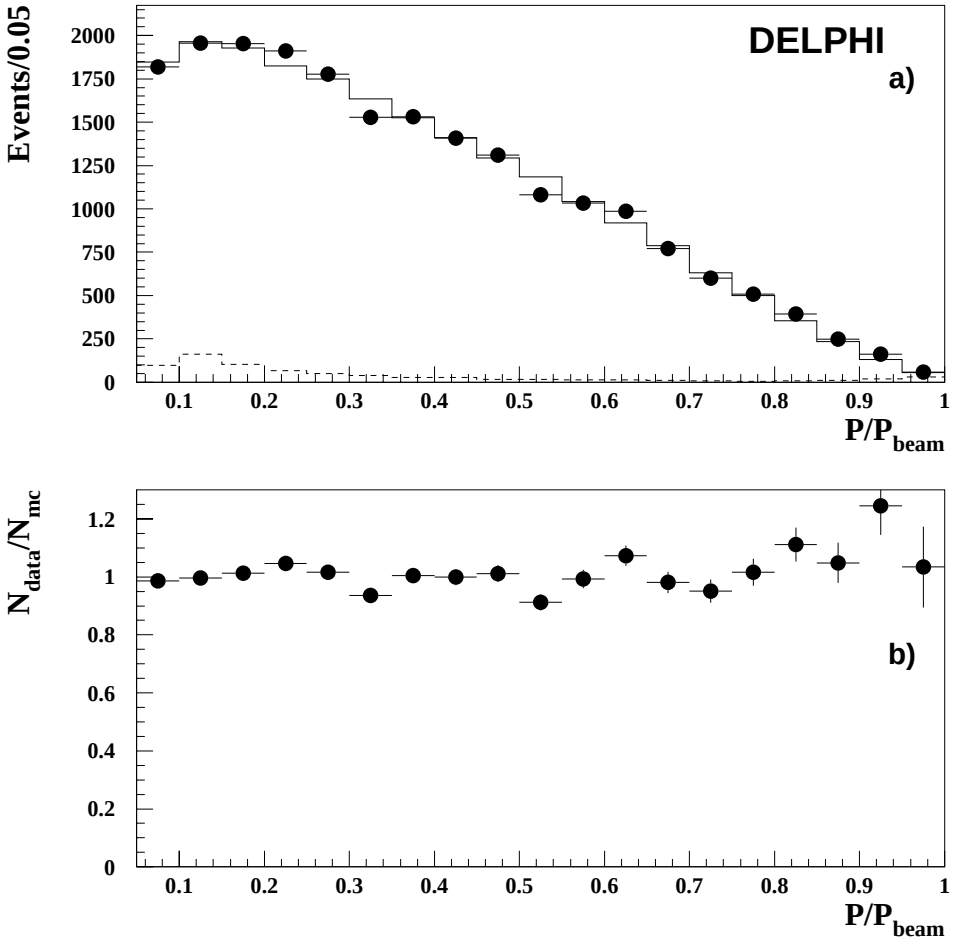

Figure 9: a) Momentum distribution of the final sample of μ candidates Points are data, solid line is the expectation from simulation. The dashed line is the expected background contribution to this. b) Shows the ratio between data and expectation as function of momentum.

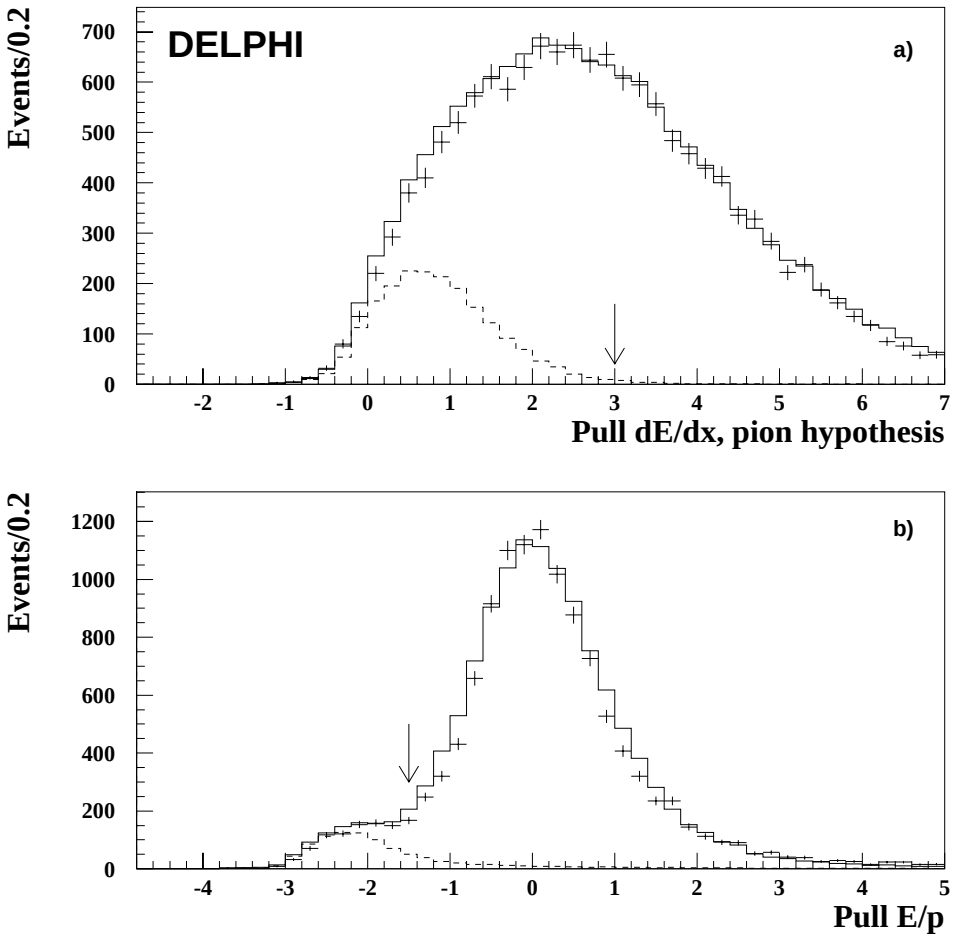

Figure 10: Variables for electron identification in the momentum range $0.05 < p/p_{beam} < 0.5$: a) $\Pi^{\pi}_{dE/dx}$, b) $\Pi_{E/P}$. Events are accepted for further analysis if at least one of the pull variables has a value above the value indicated by the arrows.

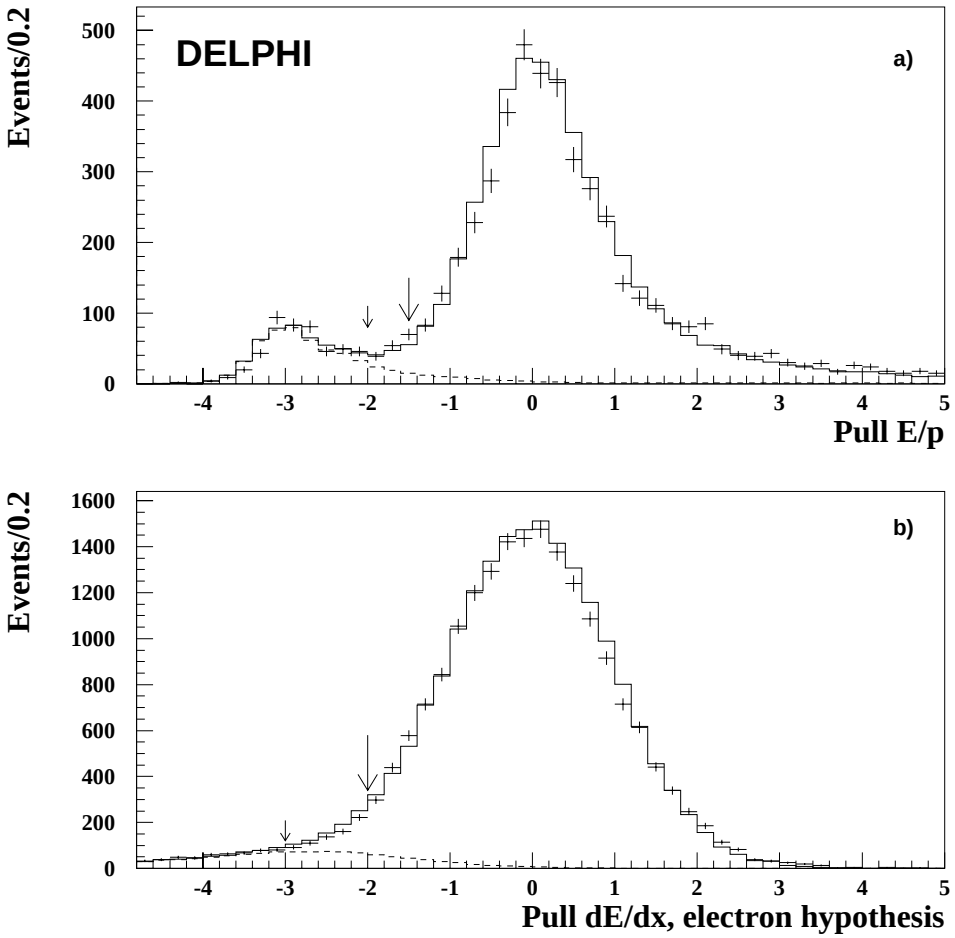

Figure 11: a) $\Pi_{E/P}$ for momenta above $0.5 \times p_{beam}$b) $\Pi^e_{dE/dx}$ for the whole event sample. Events to the right of the large arrows are accepted as electron candidates. The background contribution is normalized to fit the number of events to the left of the small arrows. The small excess in simulation around $\Pi^e_{dE/dx} = -2.$ is found to be due to the simulated response to electrons rather than due to background events.

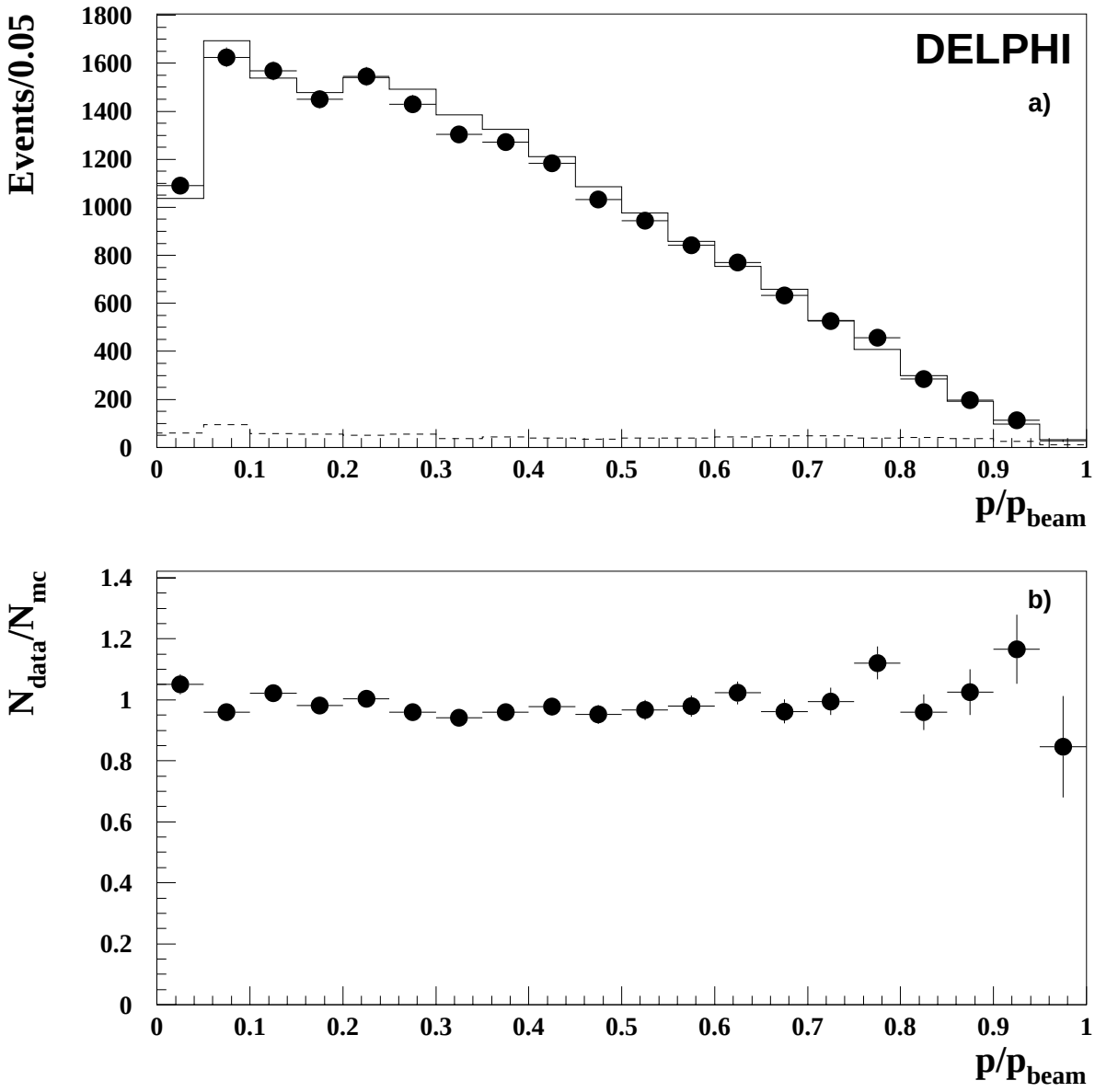

Figure 12: a) Momentum distribution for identified electrons b) the ratio between data and expectation from simulation

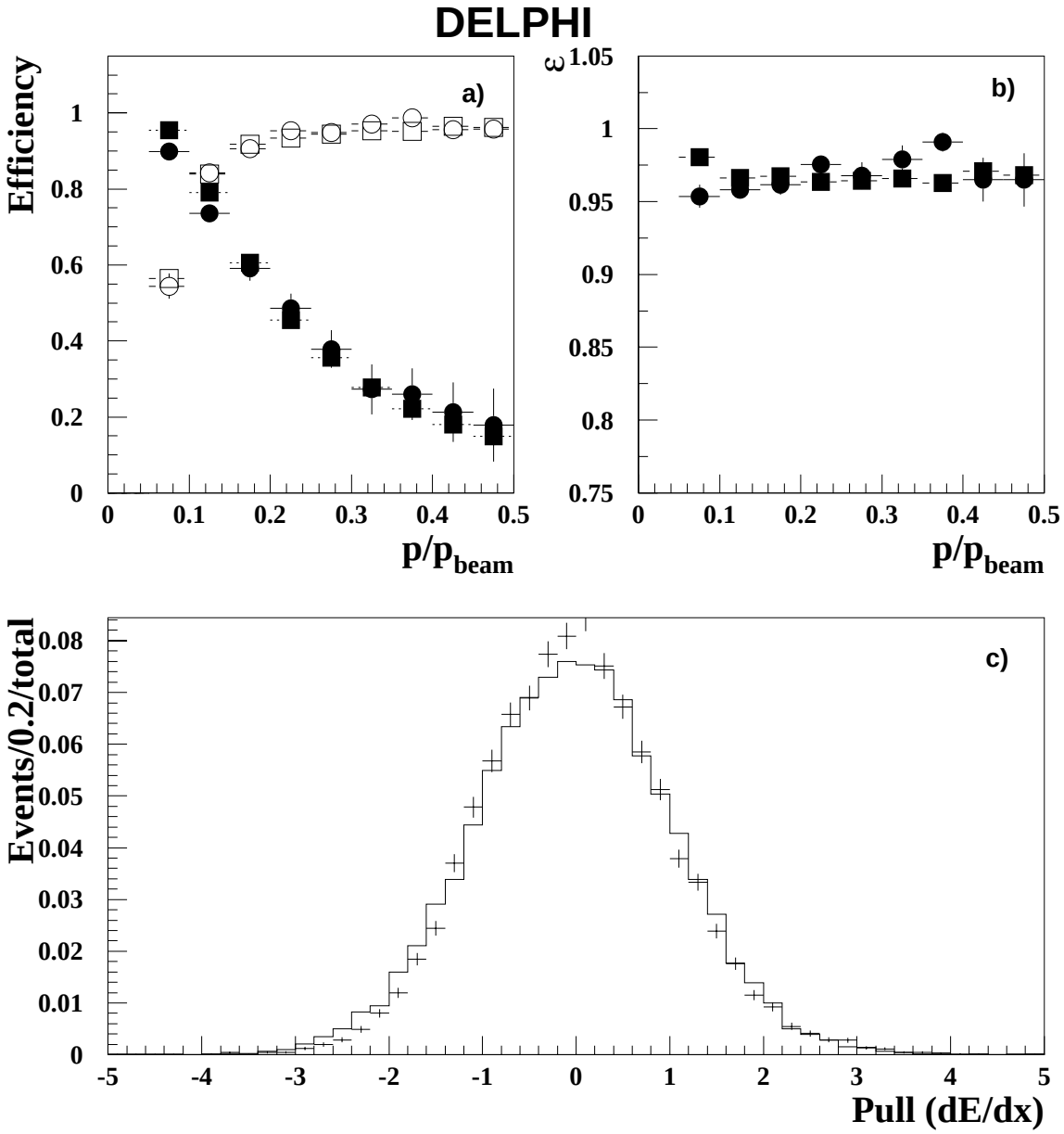

Figure 13: Example of efficiency checks, for the electron sample from 1994. a) Efficiency of the $\Pi_{E/p}$ (open marks) and $\Pi^{\pi}_{dE/dx}$ (solid marks) requirements as function of momentum. b) the efficiency estimated from the .OR. from this requirement. Circles are simulation, squares are for data. c) $\Pi^{e}_{dE/dx}$ for a selected sample of bhabhas. Crosses are data, solid line is simulation.

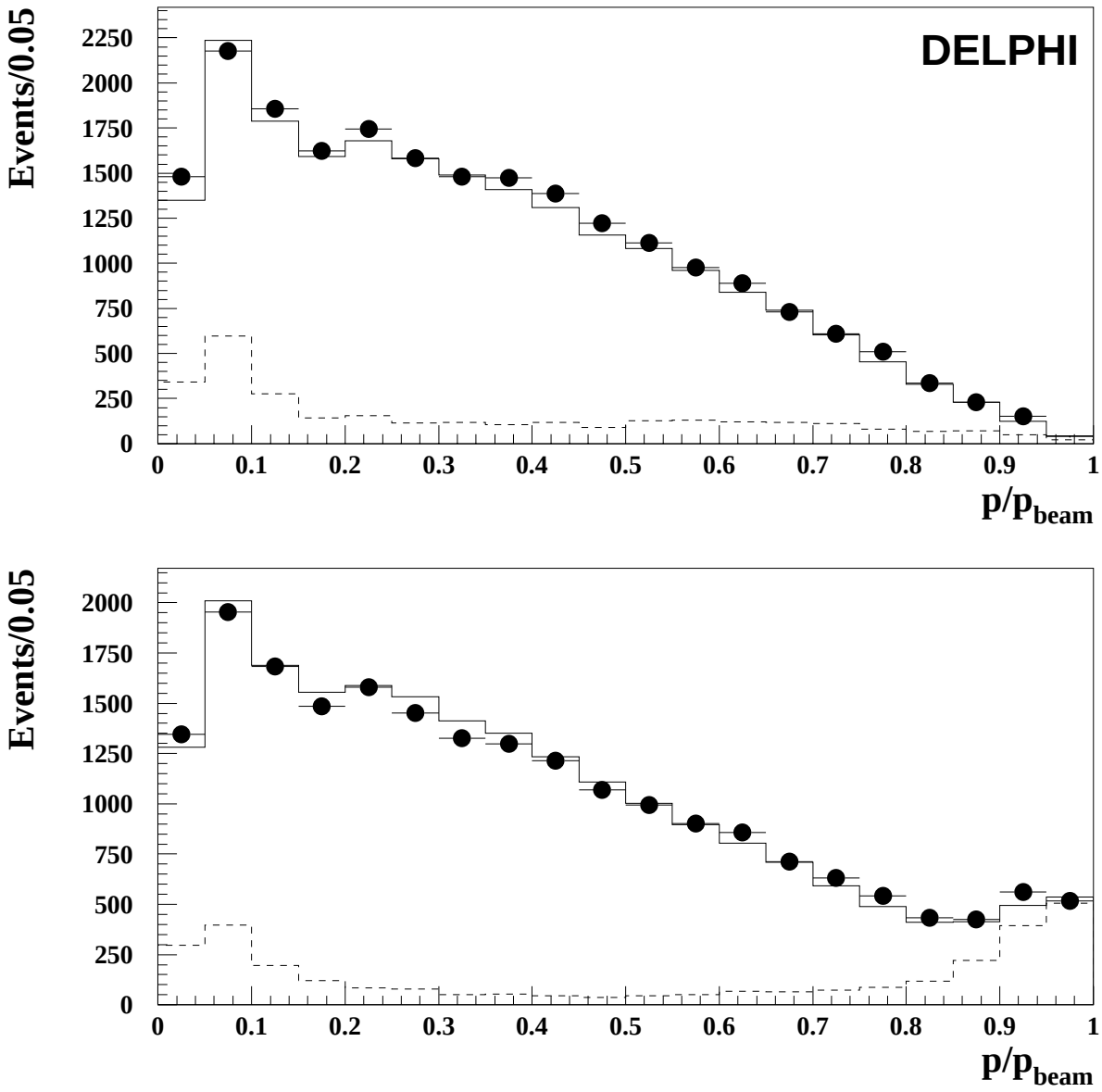

Figure 14: Momentum distribution for identified electrons a) no acollinearity cut, b) no E_{rad} cut